Magnetic instabilities in Kondo insulators

V. Dorin and P. Schlottmann

Department of Physics and Center for Materials Research and Technology, Florida State University, Tallahassee, Florida 32306

Kondo insulators such as $Ce_3Bi_4Pt_3$ and CeNiSn are small-gap semiconductor compounds. We consider a stoichiometric Kondo insulator described by the symmetric Anderson lattice without orbital degenacy and on average two electrons per site. We use a Gutzwiller-type mean-field approximation formulated in terms of four slave bosons per site in analogy with Kotliar and Ruckenstein's approach for the Hubbard model. A hybridization gap on the scale of the Kondo temperature opens in the paramagnetic phase, giving rise to the semiconducting properties at low temperatures. The paramagnetic solution is stable for sufficiently small U, but not stable with respect to a metallic ferromagnetic phase if $U > 1.54V$ (first-order transition) and antiferromagnetic long-range order for $U > 0.45V$ (second-order transition). In zero field the energy of the antiferromagnetic phase is always lower than the energy of the ferromagnetic state. Quantum fluctuations and the Ruderman-Kittel-Kasuya-Yosida interaction are expected to stabilize the paramagnetic and antiferromagnetic phases as compared to the ferromagnetic one. We also discuss the effects of a strong magnetic field.

I. INTRODUCTION

The low-temperature properties of heavy-electron systems, in particular, the development of coherence in stoichiometric compounds, have received a large amount of attention in recent years.[1,2] The coherence manifests itself most significantly in the low-temperature resistivity and magnetoresistivity. As a consequence of the translational invariance of the lattice, there is effectively no scattering (Bloch theorem) at low T and low energies, and the resistivity is then ideally zero at $T=0$ for a heavy-fermion metal.

The effects of coherence are most pronounced in so-called Kondo insulators, which have small-gap semiconductor properties. Here, as a consequence of the coherence, a hybridization gap opens at the Fermi level. The Kondo insulators SmS, SmB_6, and TmSe were already an exciting topic about ten years ago.[3] The more recent discovery of several Ce, Yb, and U Kondo insulators, e.g., CeNiSn,[4] $Ce_3Bi_4Pt_3$,[5] YbB_{12},[6] and UNiSn,[7] has renewed and enhanced the interest in this subject. All systems seem to be nonmagnetic (i.e., van Vleck dominated susceptibility) at low T, except TmSe and UNiSn for which antiferromagnetic long-range order has been reported. In UNiSn the antiferromagnetic transition is accompanied by an insulator-metal transition, so that the system is semiconducting only at higher temperatures. In view of the small energy gaps involved, the properties of these compounds strongly depend on strains in the crystal and impurities.

The formation of the coherent state in the Kondo lattice can also be studied by introducing disorder into the system,[8] i.e., by alloying nonmagnetic impurities (Kondo holes) substituting for the rare earth or actinide ions. Adding impurities to a Kondo lattice breaks the translational invariance and gradually destroys the coherence of the heavy-fermion ground state.

In recent publications[9,10] we reported a simple microscopic theory of the Kondo hole, for both the metallic and the insulating situations. In the case of a Kondo insulator a bound state (δ function in the density of states) develops in the energy gap. These states only appear in the coherent phase and disappear in the continuum at higher temperatures. When the concentration of Kondo holes is increased, an impurity band forms in the gap.[11] The effect of adding nonmagnetic impurities is then to gradually smear the hybridization gap in the Kondo insulator. For a low density of Kondo holes, the width and height of this band depend nonanalytically on the impurity concentration and the Fermi level is pinned within this band. As a consequence of this finite bandwidth there is a small low-temperature regime in which the specific heat is proportional to T and the susceptibility is finite as $T \to 0$. A metal-insulator transition is expected as a function of the Kondo-hole concentration.

Doniach and Fazekas[12] considered the formation of an antiferromagnetic ground state in a doped Kondo insulator. Again the Kondo holes introduce a band of heavy-particle excitations. They argue that the exchange coupling between the heavy particles can lead to an antiferromagnetic ground state at relatively low doping. For larger doping (dirty metal) the system may revert to a nonmagnetic state. They anticipate the possibility of a tongue of antiferromagnetic phase protruding into the nonmagnetic region of the phase diagram at low to intermediate coupling.

The formation of antiferromagnetic long-range order in heavy-fermion metals has been a subject of intensive theoretical studies.[13-17] Experimentally a faint antiferromagnetic order has been observed in several heavy-fermion metals at low temperatures. The ordered magnetic moment is very small due to the competition between the Ruderman-Kittel-Kasuya-Yosida (RKKY) interaction with the Kondo effect. For small Kondo coupling antiferromagnetic order is expected, while if J is large the ground state is paramagnetic.

In principle, a stoichiometric Kondo insulator (no Kondo holes) could also have a magnetic ground state. We address this question in this paper within a mean-field approximation for the symmetric Anderson lattice. Following Kotliar and Ruckenstein's approach[18] (for other variational treatments see Ref. 19) for the Hubbard model, we introduce four auxiliary bosons at each site, which then are replaced by scalars in the molecular field treatment. This approach is closely related to the Gutzwiller method. We analyze the paramagnetic, ferromagnetic, and antiferromagnetic solutions for the mean-field Kondo insulator. Using a bandwidth $D = 10V$, V being the on-site hybridization between f and conduction states, we obtain that the ground state is paramagnetic for small U and the antiferromagnetic phase is stable for $U > 0.45V$. A strong magnetic field lowers the energy of the ferromagnetic state, and for large fields and sufficiently large U the ground state is metallic and ferromagnetic. Quantum fluctuations about the mean-field solution are, on the one hand, believed to reduce the long-range order, while, on the other hand, the Ruderman-Kittel-Kasuya-Yosida interaction for a half-filled conduction band is expected to favor antiferromagnetism. These competing effects probably shift the para-antiferromagnetic boundary to larger-U values.

The definition of the projectors renormalizing the hybridization is not unique. There are several possible choices for the normalization of the projection operators that reproduce all matrix elements correctly. The one here is associated with the Gutzwiller approximation and reproduces the $U = 0$ limit correctly in mean field, although the approach is actually intended for highly correlated states. Within the mean-field approximation it gives a collective enhancement of the Kondo temperature and a tendency towards magnetic long-range order. This is very different from the $1/N$ slave boson approach,[20-22] which shows no collective enhancement nor magnetic order, and yields universal properties as a function of one energy scale. In both approaches fluctuations play a fundamental role: within the Gutzwiller approximation the tendency towards magnetic order and the energy scale are expected to diminish, while within the $1/N$ expansion magnetic order has to be induced (probably to order N^{-2}).

The rest of the paper is organized as follows. In Sec. II, we introduce the Anderson model and the mean-field equations for the paramagnetic, the ferromagnetic, and the antiferromagnetic situations. In Sec. III, we present the numerical solution of the equations. Concluding remarks follow in Sec. IV.

II. THE MODEL AND MEAN-FIELD APPROXIMATION

We consider the Anderson lattice without orbital degeneracy and with an on-site hybridization V. The Hamiltonian is given by

$$H = \sum_{k\sigma} \epsilon_k c_{k\sigma}^\dagger c_{k\sigma} + \epsilon_f \sum_{i\sigma} f_{i\sigma}^\dagger f_{i\sigma} + U \sum_i n_{i\uparrow} n_{i\downarrow}$$
$$+ V \sum_{k\sigma} (c_{k\sigma}^\dagger f_{k\sigma} + f_{k\sigma}^\dagger c_{k\sigma}) , \quad (2.1)$$

where ϵ_f is the f level energy, U is the Coulomb repulsion in the f shell, $n_{i\sigma} = f_{i\sigma}^\dagger f_{i\sigma}$, $c_{k\sigma}^\dagger$ ($f_{k\sigma}^\dagger$) creates a conduction electron (f electron) with momentum k and spin σ, and $f_{i\sigma}^\dagger$ is the Wannier state at the site R_i. The solution of this model is straightforward if $U = 0$. A gap opens around the f-level position ϵ_f and we have an insulator if the Fermi level lies in the gap. This corresponds to, on average, two electrons per site.

The effect of U is to introduce correlations into the system. In particular, the double occupancy of a site by two f electrons becomes unlikely for a sufficiently large U, leading to a complicated many-body problem. The constraints on the f occupation of the sites can be reformulated in terms of "auxiliary bosons."[20-22] This method has been extensively used in the $U \to \infty$ limit, where only one "slave boson" per site is needed to exclude the double occupancy. The method has been extended by Kotliar and Ruckenstein[18] to the finite-U situation by introducing four "slave bosons" per site. They studied the Hubbard model with this approach, and later Balseiro et al.[23,24] applied this slave-boson technique to a model for highly correlated bands of hybridized Cu $3d$ and O $2p$ orbitals. The Kotliar-Ruckenstein slave-boson approach has recently been developed in a spin-rotationally-invariant form.[25]

In this paper we use the non-spin-rotationally-invariant formulation of Kotliar and Ruckenstein. We introduce four Bose creation and annihilation operators for each site: $e^\dagger, e$ and $d^\dagger, d$ for the empty and doubly occupied state, and $p_\uparrow^\dagger, p_\uparrow$ and $p_\downarrow^\dagger, p_\downarrow$ for the single occupied states. These bosons act as projectors onto the corresponding electronic states. They satisfy the constraint (completeness relation)

$$e_i^\dagger e_i + p_{i\uparrow}^\dagger p_{i\uparrow} + p_{i\downarrow}^\dagger p_{i\downarrow} + d_i^\dagger d_i = 1 \quad (2.2a)$$

and the conditions

$$f_{i\uparrow}^\dagger f_{i\uparrow} = p_{i\uparrow}^\dagger p_{i\uparrow} + d_i^\dagger d_i ,$$
$$f_{i\downarrow}^\dagger f_{i\downarrow} = p_{i\downarrow}^\dagger p_{i\downarrow} + d_i^\dagger d_i . \quad (2.2b)$$

In the physical subspace defined by Eqs. (2.2), the operators $f_{i\sigma}^\dagger$ and $f_{i\sigma}$ are replaced by

$$Z_{i\sigma}^\dagger f_{i\sigma}^\dagger , \quad f_{i\sigma} Z_{i\sigma} , \quad (2.3)$$

so that the matrix elements are invariant in the combined fermion-boson Hilbert space. The constraints (2.2a) and (2.2b) are incorporated via Lagrange multipliers $\lambda_i^{(1)}$ and $\lambda_{i\sigma}^{(2)}$, respectively. The Hamiltonian now reads (B is the magnetic field)

$$H = \sum_{k\sigma} \epsilon_k c_{k\sigma}^\dagger c_{k\sigma} + \sum_{i\sigma} (\epsilon_f - \sigma B) f_{i\sigma}^\dagger f_{i\sigma} + V \sum_{i\sigma} (c_{i\sigma}^\dagger f_{i\sigma} Z_{i\sigma} + Z_{i\sigma}^\dagger f_{i\sigma}^\dagger c_{i\sigma})$$
$$+ U \sum_i d_i^\dagger d_i + \sum_i \lambda_i^{(1)} (e_i^\dagger e_i + p_{i\uparrow}^\dagger p_{i\uparrow} + p_{i\downarrow}^\dagger p_{i\downarrow} + d_i^\dagger d_i - 1) + \sum_{i\sigma} \lambda_{i\sigma}^{(2)} (f_{i\sigma}^\dagger f_{i\sigma} - p_{i\sigma}^\dagger p_{i\sigma} - d_i^\dagger d_i) . \quad (2.4)$$

As shown by Kotliar and Ruckenstein,[18] the definition of the operators $Z_{i\sigma}$ is not unique, but the following choice yields the correct matrix elements and the correct expectation value of $\langle Z_{i\sigma}^\dagger Z_{i\sigma} \rangle$ within the mean-field approximation as $U \to 0$:

$$Z_{i\sigma} = (1 - d_i^\dagger d_i - p_{i\sigma}^\dagger p_{i\sigma})^{-1/2} (e_i^\dagger p_{i\sigma} + p_{i-\sigma}^\dagger d_i)(1 - e_i^\dagger e_i - p_{i-\sigma}^\dagger p_{i-\sigma})^{-1/2} . \tag{2.5}$$

In the mean-field (saddle-point) approximation we replace all boson operators by their expectation values. For the sake of simplicity we restrict ourselves to the symmetric situation, i.e., $\epsilon_f = -U/2$ and two electrons per site. Under these circumstances,

$$\sum_\sigma \langle f_{i\sigma}^\dagger f_{i\sigma} \rangle = 1 , \quad \langle p_{i\sigma}^\dagger \rangle = \langle p_{i\sigma} \rangle = p_\sigma ,$$

$$\langle e_i^\dagger \rangle = \langle e_i \rangle = \langle d_i^\dagger \rangle = \langle d_i \rangle = d ,$$

$$\langle Z_{i\sigma} \rangle = \langle Z_{i\sigma}^\dagger \rangle = \langle Z_{i-\sigma} \rangle = \langle Z_{i-\sigma}^\dagger \rangle = Z , \tag{2.6}$$

$$Z = \frac{d(p_\sigma + p_{-\sigma})}{[(p_\sigma^2 + d^2)(p_{-\sigma}^2 + d^2)]^{1/2}} ,$$

and the mean-field Hamiltonian takes the form

$$H = \sum_{k\sigma} \epsilon_k c_{k\sigma}^\dagger c_{k\sigma} + \sum_{i\sigma} \epsilon_{f\sigma} f_{i\sigma}^\dagger f_{i\sigma} + VZ \sum_{i\sigma} (c_{i\sigma}^\dagger f_{i\sigma} + f_{i\sigma}^\dagger c_{i\sigma}) + Nd^2(U + 2\lambda^{(1)} - \lambda_\uparrow^{(2)} - \lambda_\downarrow^{(2)})$$

$$+ Np_\uparrow^2(\lambda^{(1)} - \lambda_\uparrow^{(2)}) + Np_\downarrow^2(\lambda^{(1)} - \lambda_\downarrow^{(2)}) - N\lambda^{(1)} , \tag{2.7}$$

where N is the number of sites and $\epsilon_{f\sigma} = \epsilon_f - \sigma B + \lambda_\sigma^{(2)}$ is the renormalized f-level energy. $\lambda_\sigma^{(2)}$ consists of a spin-dependent and a spin-independent term. In the symmetric situation [in order to satisfy the first condition of (2.6)] the latter is equal to $U/2$, so that $\epsilon_{f\sigma}$ changes sign with the spin, i.e., $\epsilon_{f\sigma} = -\sigma \tilde{\epsilon}_f$, where $\tilde{\epsilon}_f$ is to be determined self-consistently.

The parameters $\tilde{\epsilon}_f$, $\lambda^{(1)}$, $p_\uparrow$, $p_\downarrow$, and d are obtained by minimization of the ground-state energy of (2.7), i.e.,

$$\frac{\partial \langle H \rangle}{\partial \tilde{\epsilon}_f} = 0 , \quad \frac{\partial \langle H \rangle}{\partial \lambda^{(1)}} = 0 , \quad \frac{\partial \langle H \rangle}{\partial p_\sigma} = 0 , \quad \frac{\partial \langle H \rangle}{\partial d} = 0 . \tag{2.8}$$

The corresponding equations are

$$\langle f_{i\sigma}^\dagger f_{i\sigma} \rangle = p_\sigma^2 + d^2 , \quad p_\uparrow^2 + p_\downarrow^2 + 2d^2 = 1 ,$$

$$\frac{\partial Z}{\partial p_\sigma} V \sum_{\sigma'} \langle f_{i\sigma'}^\dagger c_{i\sigma'} \rangle + (\lambda^{(1)} - \lambda_\sigma^{(2)}) p_\sigma = 0 , \tag{2.9}$$

$$\frac{\partial Z}{\partial d} V \sum_{\sigma'} \langle f_{i\sigma'}^\dagger c_{i\sigma'} \rangle + 2\lambda^{(1)} d = 0 .$$

The parameter $\lambda^{(1)}$ can be eliminated from the last two equations, yielding

$$\left[2d \frac{\partial Z}{\partial p_\sigma} - p_\sigma \frac{\partial Z}{\partial d} \right] V \sum_{\sigma'} \langle f_{i\sigma'}^\dagger c_{i\sigma'} \rangle$$

$$= (U - 2\sigma \tilde{\epsilon}_f + 2\sigma B) p_\sigma d . \tag{2.10}$$

The expectation values $\langle f_{i\sigma}^\dagger f_{i\sigma} \rangle$ and $\langle f_{i\sigma}^\dagger c_{i\sigma} \rangle$ are straightforwardly obtained from the Green's functions

$$\langle \langle f_{k\sigma} ; f_{k\sigma}^\dagger \rangle \rangle_\omega = \frac{\omega - \epsilon_k}{(\omega + \sigma \tilde{\epsilon}_f)(\omega - \epsilon_k) - Z^2 V^2} ,$$

$$\langle \langle c_{k\sigma} ; f_{k\sigma}^\dagger \rangle \rangle_\omega = \frac{ZV}{(\omega + \sigma \tilde{\epsilon}_f)(\omega - \epsilon_k) - Z^2 V^2} , \tag{2.11}$$

via

$$\langle f_{i\sigma}^\dagger f_{i\sigma} \rangle = -\frac{1}{\pi N} \sum_k \int_{-\infty}^0 d\omega \, \text{Im} \langle \langle f_{k\sigma} ; f_{k\sigma}^\dagger \rangle \rangle_\omega ,$$

$$\langle f_{i\sigma}^\dagger c_{i\sigma} \rangle = -\frac{1}{\pi N} \sum_k \int_{-\infty}^0 d\omega \, \text{Im} \langle \langle c_{k\sigma} ; f_{k\sigma}^\dagger \rangle \rangle_\omega , \tag{2.12}$$

where Im denotes the imaginary part. For simplicity we assume a flat density of states for the conduction electrons in the energy interval $(-D, +D)$. When we evaluate the integrals we distinguish between the paramagnetic, ferromagnetic, and antiferromagnetic situations.

A. Paramagnetic ground state

In the paramagnetic phase and in the absence of an external field $\langle f_{i\sigma}^\dagger f_{i\sigma} \rangle = \frac{1}{2}$, $\tilde{\epsilon}_f = 0$ and $p_\uparrow = p_\downarrow = p$. Under these circumstances we have

$$p^2 + d^2 = \frac{1}{2} ,$$

$$8(4p^2 - 1)\ln \left| \frac{D^2}{8p^2(1 - 2p^2)V^2} \right| = \frac{UD}{V^2} . \tag{2.13}$$

The solution of these equations will be discussed in the next section.

B. Ferromagnetic ground state

We now consider the case $p_\uparrow > p_\downarrow$ and $\tilde{\epsilon}_f \neq 0$. In this situation we have

$$p_\uparrow^2 + p_\downarrow^2 + 2d^2 = 1 ,$$

$$\frac{2(p_\uparrow + p_\downarrow)^2[(p_\uparrow + p_\downarrow)^2 - 1]}{p_\uparrow p_\downarrow[1 - (p_\uparrow^2 - p_\downarrow^2)^2]} \ln \left[\frac{(1 + p_\uparrow^2 - p_\downarrow^2)(1 - p_\uparrow^2 + p_\downarrow^2)^2 D^2}{2(p_\uparrow + p_\downarrow)^2(1 - p_\uparrow^2 - p_\downarrow^2)V^2} \right] = \frac{UD}{V^2} ; \tag{2.14}$$

both equations are valid quite generally, independent of whether the system is a metal or an insulator. Two more equations are needed to completely determine the four parameters d, $\tilde{\epsilon}_f$, $p_\uparrow$, and $p_\downarrow$. These equations depend on the relative magnitude of the gap ($=2Z^2V^2/D$) and $\tilde{\epsilon}_f$, i.e., on $\Lambda=\max(\tilde{\epsilon}_f, Z^2V^2/D)$,

$$p_\downarrow^2+d^2=\frac{Z^2V^2}{2D\Lambda} \; ,$$

$$\frac{2(p_\uparrow+p_\downarrow)^2[1-p_\uparrow^2-p_\downarrow^2]}{(1+p_\uparrow^2-p_\downarrow^2)[1-p_\uparrow^2+p_\downarrow^2]^2}\frac{V^2}{D}=B+\frac{(p_\uparrow-p_\downarrow)[1-p_\uparrow^2-p_\downarrow^2][1+(p_\uparrow+p_\downarrow)^2]}{2(p_\uparrow+p_\downarrow)[1-(p_\uparrow^2-p_\downarrow^2)^2]}U \; ,$$

(2.15)

where in the last equation it is assumed that $\Lambda=\tilde{\epsilon}_f>Z^2V^2/D$, i.e., that the system is metallic. This situation can be achieved either by spontaneous ferromagnetic order or via a sufficiently strong external magnetic field B.[26]

C. Antiferromagnetic ground state

In order to study antiferromagnetic order we have to introduce a lattice with two interpenetrating sublattices which we denote with indices a and b. The kinetic energy of the conduction electrons is then formulated in terms of a nearest-neighbor hopping on that lattice. Otherwise Eqs. (2.4) and (2.5) remain valid and we continue restricting ourselves to the symmetric situation. Within the mean-field approximation we have to distinguish the expectation values of the p bosons and the f-level shifts of the two sublattices, i.e.,

$$p_\uparrow^a=p_\downarrow^b=p_\uparrow \; , \quad p_\downarrow^a=p_\uparrow^b=p_\downarrow \; ,$$

$$\left|\lambda_{a\uparrow}^{(2)}-\frac{U}{2}\right|=\left|\lambda_{b\downarrow}^{(2)}-\frac{U}{2}\right|=-\left|\lambda_{a\downarrow}^{(2)}-\frac{U}{2}\right| \quad (2.16)$$

$$=-\left|\lambda_{b\uparrow}^{(2)}-\frac{U}{2}\right|=-\tilde{\epsilon}_f \; ,$$

the procedure is otherwise similar to the one that led to (2.7). To evaluate the expectation values of the f-level occupations and the hybridization terms, we need the Green's functions. Rather than a 2×2 matrix, we now should consider a 4×4 matrix involving the two sublattices. The Brillouin zone is reduced to one-half of its original size and there are four (rather than two) bands. The energies of the bands are given by [$\epsilon=\epsilon(\mathbf{k})$ is the conduction electron dispersion]

$$\omega=\pm\tfrac{1}{2}(\tilde{\epsilon}_f^2+2V^2Z^2+\epsilon^2+2\sqrt{\epsilon^2\tilde{\epsilon}_f^2+V^4Z^4})^{1/2}$$

$$\pm\tfrac{1}{2}(\tilde{\epsilon}_f^2+2V^2Z^2+\epsilon^2-2\sqrt{\epsilon^2\tilde{\epsilon}_f^2+V^4Z^4})^{1/2} \; .$$

The band structure is schematically shown in Figs. 1(a) and 1(b). Figure 1(a) corresponds to a small f-level shift $\tilde{\epsilon}_f$ (weak antiferromagnetism). The band structure changes at about $\tilde{\epsilon}_f=0.71VZ$ to the shape shown in Fig. 1(b), which represents the strong antiferromagnetism situation. To simplify the $\mathbf{k}$ integrations, we replace the density of states of the tight-binding band of the conduction electrons by a flat density of states. After some algebra we obtain for the f density of states on the a sublattice for the majority- and minority-spin directions, respectively,

$$\rho_{a\uparrow}(\omega)=\frac{V^2Z^2}{2D}\left[\frac{\omega^2-\omega\tilde{\epsilon}_f-(VZ)^2}{[\omega^2+\omega\tilde{\epsilon}_f-(VZ)^2](\omega+\tilde{\epsilon}_f)^3(\omega-\tilde{\epsilon}_f)}\right]^{1/2}\Theta\left[D^2-\left|\frac{(\omega^2-V^2Z^2)^2-\omega^2\tilde{\epsilon}_f^2}{\omega^2-\tilde{\epsilon}_f^2}\right|\right] \; ,$$

$$\rho_{a\downarrow}(\omega)=\frac{V^2Z^2}{2D}\left[\frac{\omega^2+\omega\tilde{\epsilon}_f-(VZ)^2}{[\omega^2-\omega\tilde{\epsilon}_f-(VZ)^2](\omega-\tilde{\epsilon}_f)^3(\omega+\tilde{\epsilon}_f)}\right]^{1/2}\Theta\left[D^2-\left|\frac{(\omega^2-V^2Z^2)^2-\omega^2\tilde{\epsilon}_f^2}{\omega^2-\tilde{\epsilon}_f^2}\right|\right] \; ,$$

(2.17)

where Θ denotes the step function. The density of states $\rho_{a\uparrow}$ (majority-spin direction) for $\tilde{\epsilon}_f=0.1VZ$ is plotted in Fig. 2. The main contribution in the ω integration to obtain the expectation values arises from the dominant peak in the density of states. This can be used to greatly simplify the integration (it involves an approximation of the order of 1%) and to arrive at the following analytic self-consistency equations:

$$p_\uparrow^2+p_\downarrow^2+2d^2=1 \; ,$$

$$2(p_\uparrow^2+d^2)=1+\frac{\tilde{\epsilon}_f}{\sqrt{\tilde{\epsilon}_f^2+(V^2Z^2/D)^2}+V^2Z^2/D} \; ,$$

$$\frac{UD}{V^2}=\frac{2(p_\uparrow+p_\downarrow)^2[(p_\uparrow+p_\downarrow)^2-1]}{p_\uparrow p_\downarrow[1-(p_\uparrow^2-p_\downarrow^2)^2]}\ln\left[\frac{[1-(p_\uparrow^2-p_\downarrow^2)^2]^2D^2}{(p_\uparrow+p_\downarrow)^2(1-p_\uparrow^2-p_\downarrow^2)[\sqrt{1+3(p_\uparrow^2-p_\downarrow^2)^2}+1-(p_\uparrow^2-p_\downarrow^2)^2]V^2}\right] \; ,$$

(2.18)

$$\frac{UD}{V^2}=\frac{8(p_\uparrow+p_\downarrow)^3}{[1+(p_\uparrow+p_\downarrow)^2][1-(p_\uparrow^2-p_\downarrow^2)^2]} \; .$$
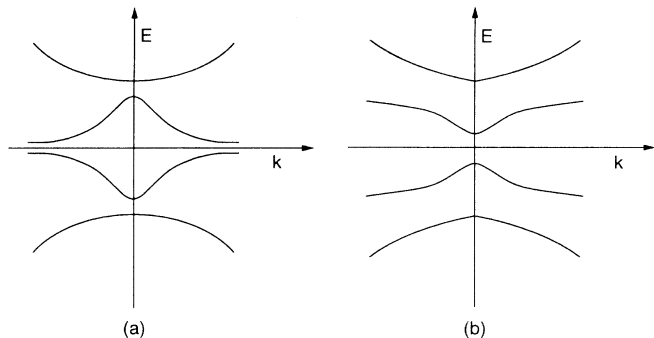
FIG. 1. Schematic band structure for the antiferromagnetic ground state. The Brillouin zone is reduced, so that there are four bands. Situation (a) corresponds to weak antiferromagnetism and (b) to strong long-range order. If $D \gg V$, the crossover between the two cases occurs at an f-level shift $\tilde{\varepsilon}_f = 0.71 VZ$.

The solution of the above equations is discussed in Sec. III.

III. RESULTS

In this section we present the solution of the mean-field equations for the paramagnetic, ferromagnetic, and antiferromagnetic phases.

A. Paramagnetic ground state

We first present the analytic solution of Eqs. (2.13) in the $U \rightarrow 0$ and $U \rightarrow \infty$ limits, and then discuss the numerical solution for the general case. For $U = 0$ we straightforwardly obtain

$$p_\uparrow = p_\downarrow = d = e = \tfrac{1}{2} , \qquad (3.1)$$

so that $Z = 1$, in agreement with the exact solution in this limit. This justifies the choice of the projectors $Z_{i\sigma}$ as given by Eq. (2.5). In the limit of large U, on the other hand, doubly occupied or empty sites are unlikely, so that d is small and p is close to 0.5; we obtain
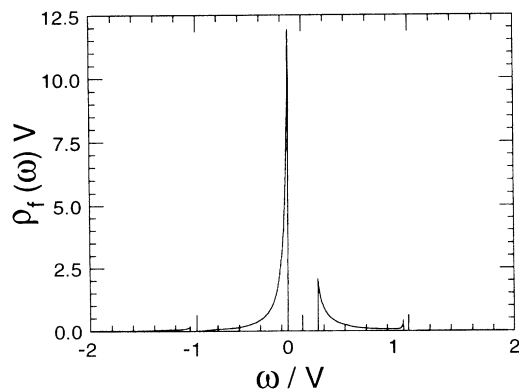

FIG. 2. f density of states for $D = 10V$ and $\tilde{\varepsilon}_f = 0.1VZ$ (corresponding to $U = 0.545V$) as a function of frequency in the antiferromagnetically ordered phase. Note that the main contribution in the ω integrations to obtain the expectation values arises from the dominant peak in the density of states.
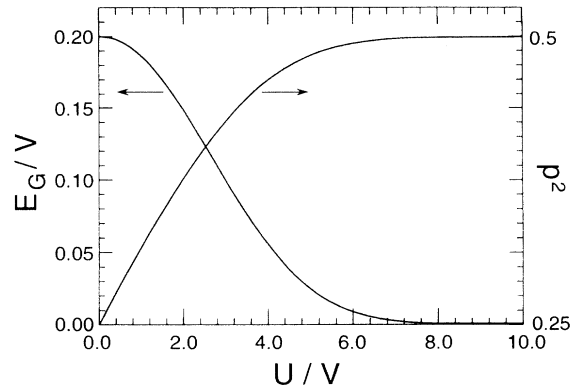

FIG. 3. Energy gap E_G and p^2 of the paramagnetic phase as a function of U/V for $D = 10V$. For $U = 0$ we have $E_G = 2V^2/D$ and $p^2 = 0.25$. In the limit $U \rightarrow \infty$ we obtain $E_G = 16d^2V^2/D$ and $p^2 = 0.5$. The large-U asymptotics, Eq. (3.2), agrees well with the numerical result for U/V larger than 6.

$$d^2 = \frac{D^2}{8V^2} \exp\left[-\frac{UD}{8V^2} \right] . \qquad (3.2)$$

The numerical solution for p^2 as a function of U/V and $D = 10V$ is shown in Fig. 3. The gap of the Kondo insulator is given by

$$E_G = 2\frac{Z^2V^2}{D} = 16p^2(1-2p^2)\frac{V^2}{D} , \qquad (3.3)$$

which becomes $E_G = 2V^2/D$ for $U = 0$ and $E_G = 16d^2V^2/D$ in the limit $U \rightarrow \infty$. A plot of E_G as a function of U/V is shown in Fig. 3. The large-U asymptotics, Eq. (3.2), agrees well with the numerical result for U/V larger than 6.

It should be pointed out that the exponential dependence for large U, i.e., (3.2), differs by a factor of 2 from the usual Kondo exponential. This different exponential dependence is characteristic of Gutzwiller-type approximations and is known as the "lattice enhancement of the Kondo effect,"[12,27] which increases the ground-state Kondo bound-state energy of the lattice with respect to that of the impurity. This difference is believed to arise due to the "coherence" in the lattice.

B. Ferromagnetic ground state

Here we first analyze the solution of Eqs. (2.14) and (2.15) in zero field. The second equation of (2.14) yields $p_\uparrow$ as a function of $p_\downarrow$ for given U, D, and V. When inserted into the second equation of the set (2.15) for $B = 0$, we determine $p_\uparrow$ and $p_\downarrow$. This solution is obtained numerically and the result is displayed in Fig. 4. For $U < V$ there is only the paramagnetic solution with $p_\uparrow = p_\downarrow$, but there is no ferromagnetic state. For $U > V$ the equations allow for two solutions (in addition to the paramagnetic one), one corresponding to a maximum and the one other to a relative minimum of the energy. The solution representing the minimum of the energy is shown in Fig. 4.

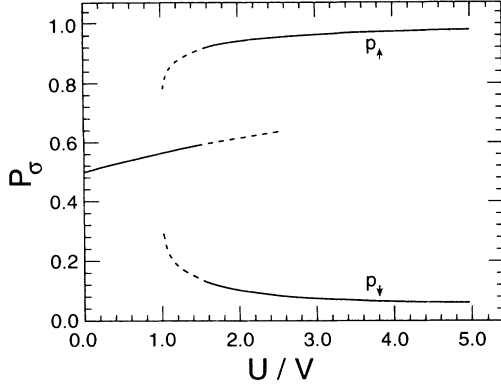Once the p_σ are determined it is straightforward to ob-

FIG. 4. $p_\uparrow$ and $p_\downarrow$ in zero field for the ferromagnetic and paramagnetic states as a function of U/V for $D = 10V$. The stable phase is indicated by the solid line and the energetically unfavorable state by the dotted line. The transition from paramagnetism to ferromagnetism at $U = 1.54V$ is of first order.

FIG. 6. Magnetization as a function of the magnetic field for various U/V values and $D = 10V$. For $U = 0$ the magnetization grows continuously when the field overcomes the energy gap. The transition is discontinuous for $U \neq 0$ and there is a spontaneous magnetization even if $B = 0$ for $U > 1.54V$.

tain the parameter d [Eq. (2.14)] for the doubly occupied and empty electronic configurations. d^2 as a function of U/V is plotted in Fig. 5. The magnetization is given by $m = p_\uparrow^2 - p_\downarrow^2$ and the energy is computed as the expectation value of H

$$E = -\frac{U}{2[(p_\uparrow + p_\downarrow)^2 - 1]}[(p_\uparrow^2 + p_\downarrow^2)^2 - (p_\uparrow - p_\downarrow)^2] .$$

(3.4)

The comparison of the energies of the paramagnetic and ferromagnetic solutions determines that the transition occurs at about $U = 1.54V$. Note that the p_σ change discontinuously, so that this transition would be of first order from a paramagnetic insulator to a metallic ferromagnet.

We follow an analogous procedure to obtain the magnetization in a finite magnetic field. Our results for m as a function of B/V for various values of U/V are displayed in Fig. 6. In zero field m is zero for $U < 1.54V$ (paramagnetic state) and, if $U > 1.54V$, there is a spontaneous magnetization. As expected the magnetization
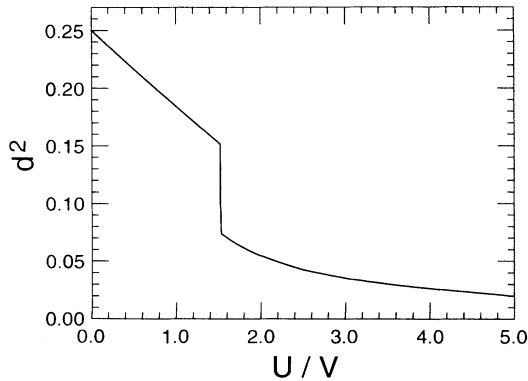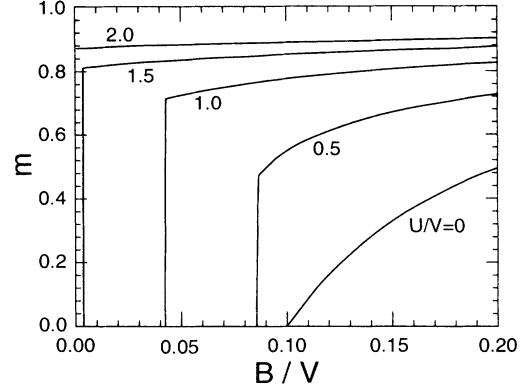
increases monotonically with the field. The critical field at which the first-order transition to a metallic ferromagnet takes place decreases with U. The transition is only continuous for $U = 0$, where the gap is closed if $B = E_G$.[26] If $U > 1.54V$, the field required to induce ferromagnetic long-range order is zero.

C. Antiferromagnetic ground state

For the antiferromagnetic ground state we proceed in a similar way as for the ferromagnet. The last two equations of set (2.18) are solved numerically to determine $p_\uparrow$ and $p_\downarrow$ (of the a sublattice) as a function of U, V, and D. The results are shown in Fig. 7 as a function of U/V and for $D = 10V$. For $U < 0.45V$ there is only the paramagnetic solution. A second solution, corresponding to an antiferromagnetic ground state, emerges for $U > 0.45V$. This is similar to the ferromagnetic situation with the exception that now the paramagnetic and antiferromagnetic solutions split continuously at $U = 0.45V$, while the two
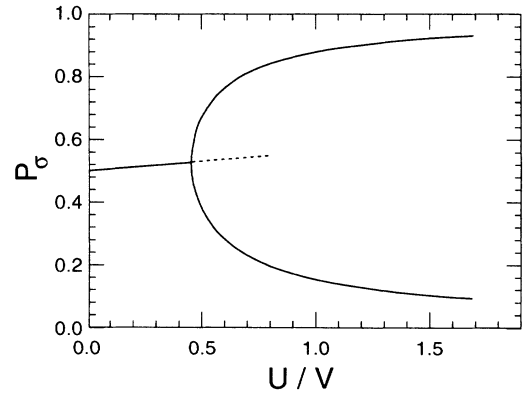

FIG. 5. Occupation probability for the doubly occupied and empty electronic configurations, d^2, as a function of U/V for $D = 10V$. For $U = 0$ we have $d = 0.5$. d decreases monotonically with U and the discontinuity indicates the transition from paramagnetism to the ferromagnetic phase.

FIG. 7. $p_\uparrow$ and $p_\downarrow$ in zero field for the antiferromagnetic and paramagnetic states as a function of U/V for $D = 10V$. The stable phase is indicated by the solid line and the energetically unfavorable state by the dotted line. The transition from paramagnetism to antiferromagnetism at $U = 0.45V$ is continuous.
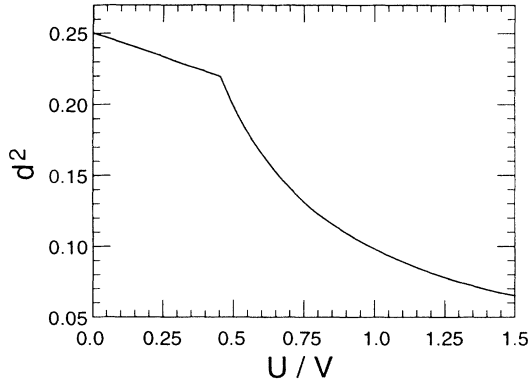
FIG. 8. Occupation probability for the doubly occupied and empty electronic configurations, d^2, as a function of U/V for $D=10V$. For $U=0$ we have $d=0.5$. d^2 decreases monotonically with U and has a kink at the transition from paramagnetism to the antiferromagnetic phase at $U=0.45V$.

solutions split discontinuously for the ferromagnet.

The energy of the antiferromagnetic ground state is also given by Eq. (3.4). The ordered state is always energetically favorable compared to the paramagnetic state. The parameter d representing the doubly occupied and empty electronic configurations is straightforwardly determined from the first equation of the set (2.18). d^2 as a function of U/V is plotted in Fig. 8. As expected d^2 decreases dramatically with increasing U. The spontaneous sublattice magnetization given by $m=p_\uparrow^2 - p_\downarrow^2$ is displayed in Fig. 9 as a function of U/V. The paramagnetic-antiferromagnetic transition is then of second order.

Next, we have to compare the ground-state energies of the two ordered phases in the parameter region where they both are stable with respect to the paramagnetic solution. It is easy to verify that the ground state always has antiferromagnetic long-range order if $U>0.45V$. The antiferromagnetic order enhances the gap of the Kondo insulator. This gap is displayed in Fig. 10 as a function of U/V.

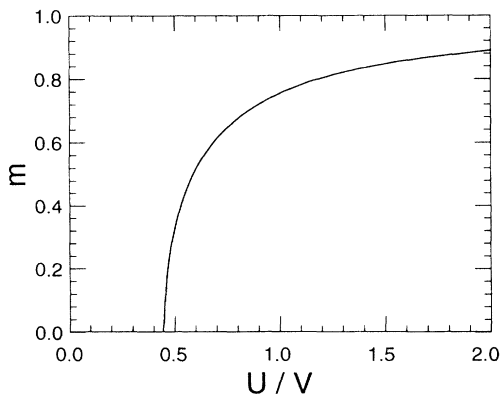We have not calculated the influence of the external

FIG. 9. Spontaneous sublattice magnetization as a function of U/V and for $D=10V$. For $U<0.45V$ the ordered magnetic moment is zero and it grows continuously with U in the antiferromagnetic phase.
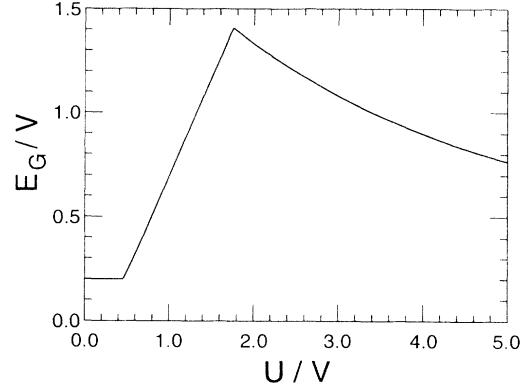

FIG. 10. Energy gap of the Kondo insulator in the paramagnetic and antiferromagnetic phases as a function of U/V for $D=10V$. The gap has two kinks: the small-U kink is the paramagnetic to antiferromagnetic transition while the other kink corresponds to the change in the band structure as discussed in Fig. 1.

magnetic field on the antiferromagnetic state. The field breaks the symmetry between the p_σ of the two sublattices, complicating the analysis. However, qualitative arguments indicate that the magnetic field interferes destructively with the antiferromagnetic long-range order, while it favors ferromagnetic long-range order. As a function of field we then expect a first-order phase transition from the antiferromagnetic solution to the ferromagnetic state. For sufficiently small U there is a first-order transition from the paramagnetic to the ferromagnetic state.

IV. CONCLUDING REMARKS

In this paper we considered a Kondo insulator as described by the symmetric nondegenerate Anderson lattice. In order to treat the correlations within the f-shell adequately, we introduced four slave bosons per site in analogy to Kotliar and Ruckenstein's treatment[18,23] of the Hubbard model. Subsequently, we performed the standard mean-field approximation and replaced the slave bosons by their expectation value. We studied the $T=0$ properties of the paramagnetic, ferromagnetic, and antiferromagnetic states as a function of U/V.

The paramagnetic solution corresponds to a Kondo insulator. It correctly reproduces the $U=0$ limit and for large U the gap has the characteristic exponential Kondo dependence. This exponential dependence includes the "lattice enhancement of the Kondo effect"[12,27] characteristic of Gutzwiller-type approximations and differs from the standard impurity Kondo temperature dependence. The many-boson approach by Kotliar and Ruckenstein is closely related to the Gutzwiller variational method, while the mean-field approximation to the single slave-boson approach (for the asymmetric Anderson lattice) by Coleman[21] and Read and Newns[22] corresponds to the leading order in a $1/N$ expansion.

In the absence of an external magnetic field the ferromagnetic state is energetically less favorable than the antiferromagnetic ground state. For $D=10V$ there is a

second-order phase transition from the paramagnetic state to the antiferromagnetically ordered one at $U = 0.45V$. The antiferromagnetic phase is insulating and the long-range order enhances the gap as compared to the paramagnetic insulating gap.

An external magnetic field breaks the symmetry between the p_σ of the two sublattices in the antiferromagnetic phase. Since the magnetic field interferes destructively with the antiferromagnetic long-range order, while it favors ferromagnetic long-range order, we expect a first-order phase transition from the antiferromagnetic solution to a ferromagnetic state for intermediate and large U. For sufficiently small U (but $U \neq 0$) there is a first-order transition from the paramagnetic to the ferromagnetic state if the field is strong enough.

If taken literally the above results would indicate that Kondo insulators are always antiferromagnets in contrast to experimental observations. Several approximations entered our calculation. First, the orbital degeneracy has been neglected. The orbital degeneracy is believed to increase the threshold for long-range order.[27] Second, Gaussian fluctuations about the mean-field approximation are also expected to reduce the antiferromagnetic order. Third, at two-loop the hybridization in the strong-coupling Anderson lattice generates a RKKY interaction between local f moments via the polarization of the conduction electrons.[28] This RKKY interaction is likely to be antiferromagnetic between nearest neighbors, and thus it again favors the instability. The interplay of the above effects is expected to raise the threshold value of U for antiferromagnetic order. Fourth, the normalization of the Z_σ factors is chosen to reproduce the weak-coupling limit, rather than the unknown strong-coupling limit for which the approach is intended for.

ACKNOWLEDGMENT

[1]G. R. Stewart, Rev. Mod. Phys. **56**, 755 (1984).

[2]P. A. Lee, T. M. Rice, J. W. Serene, J. L. Sham, and J. W. Wilkins, Comments Condens. Matter Phys. **12**, 98 (1986).

[3]See, e.g., *Valence Instabilities,* edited by P. Wachter and H. Boppart (North-Holland, Amsterdam, 1982).

[4]T. Takabatake, Y. Nakazawa, and M. Ishikawa, Jpn. J. Appl. Phys. Suppl. **26**, 547 (1987).

[5]M. F. Hundley, P. C. Canfield, J. D. Thompson, Z. Fisk, and J. M. Lawrence, Physica B **171**, 254 (1991).

[6]M. Kasaya, F. Iga, M. Takigawa, and T. Kasuya, J. Magn. Magn. Mater. **47&48**, 429 (1985).

[7]N. Bykovetz, W. H. Herman, T. Yuen, C. Jee, C. L. Lin, and J. E. Crow, J. Appl. Phys. **63**, 4127 (1988).

[8]N. B. Brandt and V. V. Moschalkov, Adv. Phys. **33**, 373 (1984).

[9]R. Sollie and P. Schlottmann, J. Appl. Phys. **69**, 5478 (1991).

[10]R. Sollie and P. Schlottmann, J. Appl. Phys. **70**, 5803 (1991).

[11]P. Schlottmann, Phys. Rev. B **46**, 998 (1992).

[12]S. Doniach and P. Fazekas, Philos. Mag. B **65**, 1171 (1992).

[13]S. Doniach, Physica B **91**, 231 (1977).

[14]C. Lacroix and M. Cyrot, Phys. Rev. B **20**, 1969 (1979).

[15]N. Read, D. M. Newns, and S. Doniach, Phys. Rev. B **30**, 3841 (1984).

[16]S. Doniach, Phys. Rev. B **35**, 1814 (1987).

[17]P. Fazekas and E. Müller-Hartmann, Z. Phys. B **85**, 285 (1991).

[18]G. Kotliar and A. Ruckenstein, Phys. Rev. Lett. **57**, 1362 (1986).

[19]B. H. Brandow, Phys. Rev. B **33**, 215 (1986).

[20]S. E. Barnes, J. Phys. F **6**, 1375 (1976); **7**, 2637 (1977).

[21]P. Coleman, Phys. Rev. B **29**, 3035 (1984).

[22]N. Read and D. M. Newns, J. Phys. C **16**, 3273 (1983).

[23]C. A. Balseiro, M. Avignon, A. G. Rojo, and B. Alascio, Phys. Rev. Lett. **62**, 2624 (1989).

[24]A. Sudbo and A. Houghton, Phys. Rev. B **42**, 4105 (1990).

[25]T. Li, P. Wölfle, and P. Hirschfeld, Phys. Rev. B **40**, 6817 (1989).

[26]A. Millis, in *Physical Phenomena at High Magnetic Fields,* edited by E. Manousakis, P. Schlottmann, P. Kumar, K. Bedell, and F. Mueller (Addison-Wesley, Reading, MA, 1991), p. 146.

[27]T. M. Rice and K. Ueda, Phys. Rev. Lett. **55**, 995 (1985).

[28]A. Houghton, N. Read, and H. Won, Phys. Rev. B **35**, 5123 (1987).